LWT - Food Science and Technology 183 (2023) 114904

Contents lists available at ScienceDirect

LWT

journal homepage: www.elsevier.com/locate/lwt

Amylose and amylopectin contents affect OSA-esterified corn starch's solubilizing efficacy and action mode on hesperetin

Feng Cao [a,b], Meiyu Zheng [a], Lu Wang [a,c], Hanyu Lu [a], Yangguang Wang [c,*], Siew Young Quek [d,e], Shengmin Lu [a,b,c,**]

[a] State Key Laboratory for Managing Biotic and Chemical Threats to the Quality and Safety of Agro-products, Zhejiang Provincial Key Laboratory of Fruit and Vegetables Postharvest and Processing Technology, Ministry of Agriculture and Rural Affairs Key Laboratory of Post-Harvest Handling of Fruits, Institute of Food Science, Zhejiang Academy of Agricultural Sciences, Hangzhou, 310021, China
[b] College of Food Science and Technology, Nanjing Agricultural University, Nanjing, 210095, China
[c] College of Food and Pharmacy, Zhejiang Ocean University, Zhoushan, 316022, China
[d] Food Science, School of Chemical Sciences, The University of Auckland, Auckland, 1010, New Zealand
[e] Riddet Institute, Centre of Research Excellence for Food Research, Palmerston North, 4474, New Zealand

ARTICLE INFO

Keywords:
Amylose
Amylopectin
Octenyl succinic anhydride modified starch
Hesperetin
Solubilization

ABSTRACT

In order to investigate the solubilization effect and action mode of octenyl succinic anhydride (OSA) modified starches with different amylose and amylopectin compositions on hesperetin (HTN), four OSA-esterified corn starches (OSAS) were prepared using the aqueous phase method. Results revealed that all OSAS could improve the solubility of HTN. OSA-High amylose starch (OSA-HAS) had the best solubility for HTN, nearly fivefold that of free HTN, while OSA-Waxy starch (OSA-WS) had the least solubility for HTN, only twofold that of free HTN. Furthermore, FT-IR, XRD, DSC, and ^{1}H NMR demonstrated the formation of complexes and the interactions between OSAS and HTN in the complexes. The results of DSC revealed that HTN and OSAS formed complexes with greater thermal stability. ^{1}H NMR disclosed that the OSA group in the OSA-HAS complex was actively involved in the interaction with HTN. However, in the OSA-WS complex, the starch backbone reacted more with HTN than the OSA group. This study expanded the knowledge on solubilizing HTN by OSA-modified starch and promoted the development of efficient solubilizing or delivery carriers for HTN, thus contributing to the sufficient utilization of citrus flavonoids.

1. Introduction

Hesperidin is an important citrus flavonoid, extensively present in citrus fruits, mainly in the pericarps. Hesperetin (HTN) is an aglycon, the main hydrolytic product of hesperidin, and has been discovered to have excellent biological and pharmacological activities, such as anticancer (Lazer et al., 2018), anti-inflammatory (Zheng, Lu, & Xing, 2021), antioxidative activity (Vaz, Jitta, Verma, & Kumar, 2021; Zheng et al., 2021), etc. However, its poor water solubility greatly restricts the application of HTN in food, pharmaceuticals, and other industries. Therefore, plenty of attentions have been put by researchers and product developers to exploring appropriate means to overcome this defect. According to the literature, there are numerous strategies to improve the solubility of flavonoids such as HTN, as indicated below.

It has been reported that cyclodextrin (CD) and its derivatives could improve the solubility of flavonoids by incorporating them into the cavities of CD and its derivatives, with the sulfobutyl ether β-cyclodextrin demonstrating the highest solubilization effect on flavonoids (You et al., 2018). In addition, *Astragalus* polysaccharides could significantly improve the solubility of flavonoids, with an increase of 68.88 folds found in quercetin (Liu et al., 2020). The melt-quenched particles of naringenin/hesperetin (1:1 in molar ratio) prepared by the melt-quenching method showed significantly improved dissolution properties of both naringenin and HTN in aqueous media (Uchiyama, Ando, Kadota, & Tozuka, 2021). It was discovered that β-CD and hydroxy-propyl-β-CD improved the solubility of HTN by 30- and 467-fold, respectively (Lucas-Abellán et al., 2019), and the solubility of HTN increased with the increasing concentrations of β-CD at gradually

* Corresponding author.
** Corresponding author. Institute of Food Science, Zhejiang Academy of Agricultural Sciences, Hangzhou, 310021, China.
E-mail addresses: 634449563@qq.com (Y. Wang), lushengmin@hotmail.com (S. Lu).

https://doi.org/10.1016/j.lwt.2023.114904
Received 26 December 2022; Received in revised form 15 May 2023; Accepted 22 May 2023
Available online 25 May 2023
0023-6438/© 2023 The Authors. Published by Elsevier Ltd. This is an open access article under the CC BY-NC-ND license (http://creativecommons.org/licenses/by-nc-nd/4.0/).

rising temperatures (Tommasini et al., 2004). Apart from the cyclodextrins and their derivatives mentioned above, octenyl succinic anhydride (OSA) is frequently employed to improve the solubility of hydrophobic active compounds.

OSA has strong hydrophobic properties and can esterify with starch to form amphiphilic OSA-modified starch (OSAS), the only FDA-approved octenyl esterified starch in food (Altuna, Herrera, & Foresti, 2018). OSAS possesses great stabilit and high encapsulation efficiency (Hh, Hz, El, Cheng, & Peng, 2019; Zhao et al., 2018), and can be used as an emulsifier, encapsulation agent, and solubilizer (Altuna et al., 2018). Studies had shown that OSAS greatly enhanced the solubility of encapsulated hydrophobic bioactive compounds like curcumin and β-carotene (Fang, Zhao, Liu, Liang, & Yang, 2019; Paramera, Konteles, & Karathanos, 2011). Abbas, Bashari, Akhtar, Wei, and Zhang (2014) prepared OSAS to stabilize curcumin nanoemulsions with an ultrasound-assisted method. Furthermore, succinylated nanoparticles from normal, high-amylose, and high-amylopectin corn starches could be employed as carriers of anthocyanin, but their encapsulation efficiencies on anthocyanin were different (Escobar-Puentes, Gurrola, Rincón, Zepeda, & Martínez-Bustos, 2020). Pickering emulsions stabilized with OSA-modified starch nanoparticles were also investigated as a delivery system for polyphenol rutin (Kuzhithariel Remanan & Zhu, 2022). These studies have indicated that OSA-modified starches may encapsulate or solubilize hydrophobic bioactive compounds.

In particular, researchers in our laboratory have done some work on solubilizing naringin, HTN and hesperidin (Guo et al., 2018; Guo, Lu, Liu, Tang, & Tu, 2019; Xiang et al., 2021). It was found that OSA-esterified waxy corn starch with different molecular weights had different solubilizing effects on naringin (Xiang et al., 2021). In addition, starches of different sources had different influence on solubility of HTN, among which corn starch was found to have the best solubilizing effect, which indicated that the composition and structure of starch affected the solubilizing ability of OSAS on HTN (Guo et al., 2018). The ratio of amylose and amylopectin is an important factor influencing starch properties, such as the solubilizing effects on HTN.

To elucidate how the amylose and amylopectin compositions in OSAS affect the solubilization of HTN, four OSA-modified corn starches with different amylose and amylopectin compositions were prepared, and those with the highest and lowest solubilizing efficacy on HTN were selected to investigate the interaction between OSAS and HTN using Fourier transform infrared spectroscopy (FT-IR), X-ray diffraction (XRD), differential scanning calorimetry (DSC), and ^{1}H nuclear magnetic resonance (^{1}H NMR). The results of this study would provide a theoretical basis for the efficient solubilization of OSA-esterified starch and the utilization of HTN, as well as promote the healthy development of citrus-related industries.

2. Materials and methods

2.1. Materials

Corn starch (CS), waxy corn starch (WS), amylose corn starch (AS), and high amylose corn starch (HAS) were purchased from Shanghai Naijin Trading Co., Ltd. (Shanghai, China). Octenyl succinic anhydride (purity ≥ 99.5%) was purchased from Jinan Haohua Industrial Co., Ltd. (Shandong, China). Hesperetin (purity ≥ 98%) was obtained from Xi'an Tianben Technology Co., Ltd. (Xi'an, China). Methanol (chromatographically pure), acetic acid and anhydrous ethanol (analytical grade) were purchased from Sigma Aldrich Co., Ltd. (St. Louis, MO, USA). Dimethyl sulfoxide (DMSO), hydrochloric acid (HCl) and sodium hydroxide (NaOH) were bought from Shanghai Sinopharm Chemical Reagent Co., Ltd. (Shanghai, China). Pure water with electronic conductivity of 2–3 × 10^{-4} S/m, obtained by the two-stage reverse osmosis process, was purchased from Hangzhou Wahaha Group Co., Ltd. (Zhejiang, China).

2.2. Determination of amylose and amylopectin contents

The dual-wavelength iodine binding technique was adopted to determine starch's amylose and amylopectin contents (Zhu, Jackson, Wehling, & Geera, 2008). Briefly, the standard solution of amylose or amylopectin (1 mg/mL) was prepared at 80 °C and added with a few drops of iodine respectively. The mixture was scanned using the UV spectrophotometry (UV1800, Shimadzu Instrument Co., Ltd., Jiangsu, China) in the range of 400–800 nm. The amylose and amylopectin contents in samples were determined at the selected wavelengths of 499 nm and 540 nm with respective reference wavelengths of 586 nm and 725 nm.

$$\triangle A_{\ amylose} = A_{586\ nm} - A_{499\ nm} \quad (1)$$

$$\triangle A_{\ amylopectin} = A_{540\ nm} - A_{725\ nm} \quad (2)$$

where $\triangle A_{\ amylose}$ and $\triangle A_{\ amylopectin}$ represent the difference in absorbance of amylose and amylopectin, respectively. $A_{586\ nm}$, $A_{499\ nm}$, $A_{540\ nm}$ and $A_{725\ nm}$ stand for the absorbance at 586 nm, 499 nm, 540 nm and 725 nm.

2.3. Preparation of OSA-modified starch

The preparation of OSA-modified starch with different amylose and amylopectin composition was conducted according to Guo et al. (2020) with slight modification. Starch slurry (0.35 g/mL) was stirred in a water bath at 35 °C, and its pH was adjusted to 8.5 using 0.5 mol/L NaOH. OSA (3%, based on dry starch weight) diluted five times with absolute alcohol (v/v) was slowly added to the starch slurry within 2 h under constant stirring and pH at 8.5 (adjusted with NaOH solution). The mixture was continuously stirred for 5 h while maintaining the constant pH value. After the reaction, the mixture was centrifuged (25 °C, 1776 g, 15 min). The precipitate was washed with distilled water for three times, followed by rinsing with 70% ethanol for three times, and then dried in an oven at 40 °C. The solid was undergone by crushing and passing through a 100-mesh sieve (the mesh size is 0.15 mm) to obtain the OSAS samples. The OSAS samples were coded as OSA-CS, OSA-WS, OSA-AS, OSA-HAS according to the name of starch used, respectively.

2.4. Determination of degrees of substitution of OSA-modified starch

The determination of the degrees of substitution (DS) of OSAS was performed according to the method of (Klaochanpong, Puncha-Arnon, Uttapap, Puttanlek, & Rungsardthong, 2017).

2.5. Determination of molecular weight of OSA-modified starch

The determination of molecular weight (Mw) of OSAS was performed according to the method of Lin et al. (2016).

2.6. Preparation of OSAS and HTN complexes and their physical mixtures

Preparation of OSAS and HTN complexes (OSAS-HTN) were performed according to the method of Guo et al. (2019). Four different OSAS solutions were prepared at 0.04 g/mL using distilled water as solvent, respectively. Then the same mass HTN as the OSAS powder was added directly to the solution with constant stirring at room temperature. After 4 h, the reaction mixtures were centrifuged at 1776 g for 15 min to collect the supernatants, followed by lyophilization to obtain the samples. A fraction of each supernatant was reserved for the determination of HTN. In addition, the physical mixtures were prepared by grinding a 1:1 mass ratio of solid mixture of HTN and one of OSAS in an agate mortar for 5 min.

2.7. Determination of hesperetin

The HTN content in the OSAS-HTN complexes were determined by a HPLC instrument (LC-2030C, SHIMADZU, Japan) using a Shim-pack GIST C_{18} column (150 mm × 4.6 mm × 5 μm). HTN standard solutions (50, 100, 150, 200, 250, 300, 350, 400, 450 μg/mL) were prepared with methanol. The mobile phases used were 0.2% acetic acid (A) and methanol (B). The isocratic elution was performed with 45% A and 55% B. The flow rate, injection amount, column temperature, and detection wavelength were 1 mL/min, 10 μL, 25 °C, and 287 nm, respectively. The supernatant of OSAS-HTN complexes was filtered through a 0.45 μm filter membrane before injection. The linear regression equation of the standard curve was obtained (Equation (3)). The HTN content in the samples was calculated according to the standard curve equation.

$$Y = 24889.69146x + 77619.0379 \ (R^2 = 0.99978) \quad (3)$$

where Y and x represent the HPLC map peak area and hesperetin concentration (μg/mL), respectively.

2.8. FT-IR spectra analysis

The FT-IR spectra of all samples were obtained using a Bruker FT-IR spectrometer (Vertex 70, Bruker Instrument Co., Ltd., Germany). The relevant dried samples were separately mixed with potassium bromide and then tableted. The spectra were collected at a resolution of 4 cm^{-1} and scanning wavelength ranging from 400 to 4000 cm^{-1} (Zhang et al., 2022).

2.9. XRD analysis

The XRD patterns were recorded with a X' Pert PRO powder diffractometer (PANalytical, Netherlands) using Cu Kα radiation (λ = 0.1541 nm). The working voltage was 40 kV, and the working current was 40 mA. The patterns were collected with a 2θ range from 5° to 60° at a step of 0.0167° (Ji et al., 2022).

2.10. Thermal property analysis

Each sample (approximately 10 mg) was put in an aluminum crucible. The thermal property measurements of samples were performed with a differential scanning calorimeter (SAT449C, NETZSCH Co., Ltd., Germany) at a heating rate of 10 °C/min from 40 °C to 400 °C in a dynamic nitrogen atmosphere (Xiang et al., 2021).

2.11. ^{1}H NMR spectra determination

The ^{1}H NMR spectra of the samples were measured on a Bruker Avance III 500M NMR spectrometer (Bruker Instrument Co., Ltd., Germany) at 500 MHz (zg30 pulse, 128 scans). All the powder samples were dissolved in DMSO-d_6, and the chemical shifts were presented in the form of δ (ppm) (Li et al., 2020).

2.12. Statistical analysis

All experiments were conducted in triplicate, and the results were expressed as mean ± standard deviation. The results were analyzed by SPSS.21.0 (SPSS Inc., Chicago, IL, USA), Origin 2021b (Origin Lab Inc., Northampton, MA, USA) and Excel 2016. The data were all analyzed using the ANOVA test, and differences between means were compared using Duncan's test with significance at $P < 0.05$. The ^{1}H NMR data were plotted using the MestReNova 14.0 (Mestrelab Research Co., Spain).

Table 1
Amylose and amylopectin contents in four corn starches.

Samples	Amylose content (%)	Amylopectin content (%)
CS	22.33 ± 0.73^{b}	27.97 ± 3.14^{c}
WS	3.62 ± 0.28^{d}	81.23 ± 1.09^{a}
AS	17.03 ± 3.35^{c}	61.49 ± 1.09^{b}
HAS	63.21 ± 1.69^{a}	19.22 ± 1.86^{d}

CS: corn starch; WS: waxy corn starch; AS: amylose corn starch; HAS: high amylose corn starch. The data were repeated three times and expressed as mean ± standard deviation. Different letters in the same column indicate significant differences between samples ($P < 0.05$).

Table 2
Degrees of substitution (DS) and molecule weight (Mw) of octenyl succinic anhydride (OSA) modified starches.

Samples	DS	Mw (kDa)
OSA-CS	0.0140 ± 0.0007^{a}	$7.0839 \pm 0.6364 \times 10^{4b}$
OSA-WS	0.0060 ± 0.0006^{c}	$12.7143 \pm 1.4991 \times 10^{4a}$
OSA-AS	0.0091 ± 0.0002^{b}	$7.6090 \pm 1.1314 \times 10^{4b}$
OSA-HAS	0.0141 ± 0.0002^{a}	$0.8952 \pm 0.0566 \times 10^{4c}$

CS: corn starch; WS: waxy corn starch; AS: amylose corn starch; HAS: high amylose corn starch. The data were repeated three times and expressed as mean ± standard deviation. Different letters in the same column indicate significant differences between treatments ($P < 0.05$).

3. Results and discussion

3.1. Amylose and amylopectin contents in starches

The amylose and amylopectin contents of all four starch samples showed significant differences (Table 1). HAS, CS, AS and WS showed a descending trend in amylose content, but were in an ascending order of amylopectin content. A study indicated that the corn amylose starch (amylose content ≥ 72%) and dihydromyricetin could spontaneously form host-guest complexes in water, that is, dihydromyricetin could spontaneously and rapidly enter the amylose spiral through non-covalent interaction (Geng, Liu, Ma, Liu, & Liang, 2021). In addition, the potato amylose (essentially free of amylopectin) could form a single helical hydrophobic cavity to encapsulate and protect catechin (Wang et al., 2021). The linear structure of amylose can form non-covalent clathrates with small molecules in food. During the formation of clathrates, amylose will own left-handed single helices with a relatively hydrophilic appearance and hydrophobic spiral channels to accommodate visitor molecules. As a consequence, it can be guessed that high amylose in OSAS possesses more helical cavities to load HTN, which spontaneously forms host-guest complexes with HTN in water, thus enhancing the solubility of HTN.

3.2. Degrees of substitution and molecule weight of OSAS

DS is expressed as the number of hydroxyl groups substituted per glucose unit. Table 2 shows the trends in DS and Mw of OSAS samples, respectively, i.e., for OSAS, the higher content of amylose and the lower content of amylopectin, the higher its DS value and the lower its Mw, which was consistent with the reported lower molecular weight found in amylose than amylopectin (Obadi, Qi, & Xu, 2022). The results suggested that amylose is more easily esterified by OSA than amylopectin. Therefore, OSA-WS owned the lowest DS (0.0060) and the highest Mw ($12.7143 \pm 1.4991 \times 10^4$ kDa), whereas OSA-HAS had the highest DS (0.0141) and the lowest Mw ($0.8952 \pm 0.0566 \times 10^4$ kDa). The higher DS means that starch reacts with OSA more thoroughly, and OSAS owns more amphiphilicity (Wang et al., 2022). Previous studies have revealed that the esterification of OSA mainly occurs in the amorphous region of starch, which is usually composed of amylose (Klaochanpong et al., 2017; Shogren, Viswanathan, Felker, & Gross, 2000). This is why

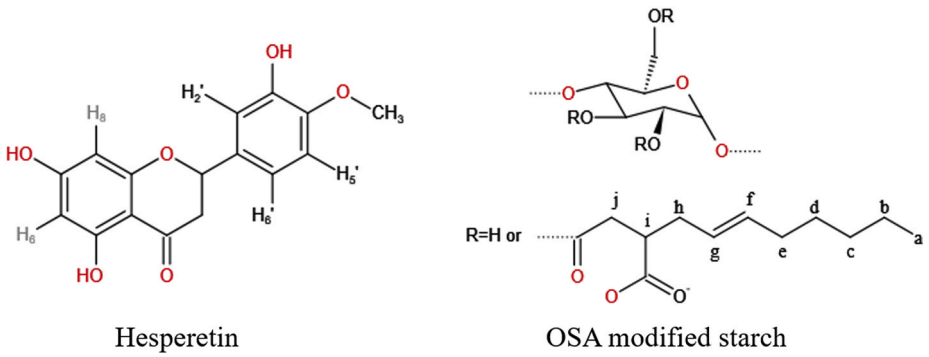

Fig. 1. Chemical structures of hesperetin and octenyl succinic anhydride (OSA) modified starch.

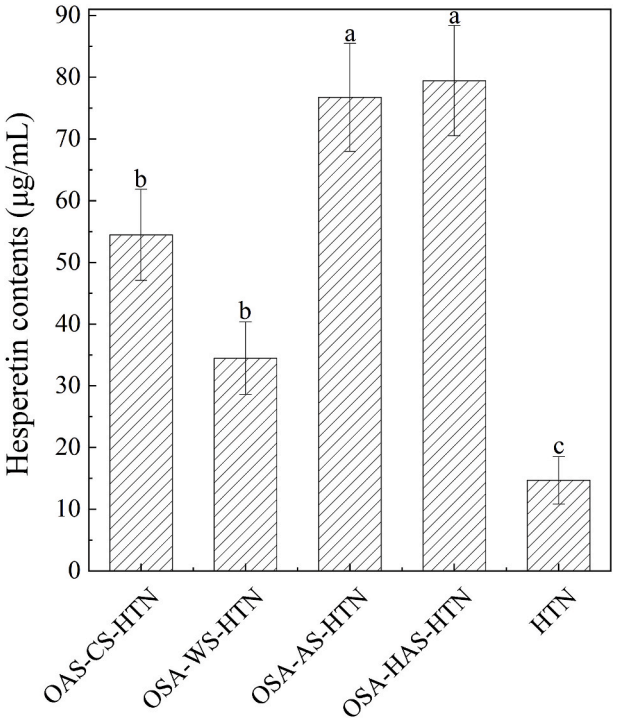

Fig. 2. Hesperetin contents in OSAS-HTN complexes and free hesperetin. OSA: octenyl succinic anhydride; HTN: hesperetin; CS: corn starch; WS: waxy corn starch; AS: amylose corn starch; HAS: high amylose corn starch. The data were repeated three times and expressed as mean ± standard deviation. Different letters on tops of the column graphs indicate significant difference between samples ($P < 0.05$).

OSA-HAS has the highest DS and thus results in better amphiphilicity, which is supposed to bind more HTN and has a better solubilization effect on HTN.

3.3. *Effect of the amylose and amylopectin composition in OSAS on solubility of hesperetin*

For the OSAS-HTN complexes, OSA-WS with the lowest amylose content loaded the least HTN (34.49 μg/mL), while OSA-HAS with the highest amylose content loaded the highest amount of HTN (79.44 μg/mL) (Fig. 2). As a control, the water solubility of free HTN was determined to be only 14.71 μg/mL. The amylose/amylopectin contents of AS and HAS were significantly different, while the HTN contents in OSA-AS-HTN and OSA-HAS-HTN were not significantly different. This might be due to the significant difference in Mw between OSA-AS ($7.6090 \pm 1.1314 \times 10^4$ kDa) and OSA-HAS ($0.8952 \pm 0.0566 \times 10^4$ kDa). It was discovered that the Mw of OSAS had a substantial effect on the amount of naringin embedded in the complex of OSAS and naringin, and OSAS with a higher Mw showed higher naringin loading (Xiang et al., 2021). Therefore, OSA-AS with higher Mw could load more HTN. The increase of HTN content in OSAS-HTN complexes indicated the solubilization effect of OSAS on HTN. The incorporation of OSA into starch provides part of the hydrophobic branch chains to hydrophilic starch and makes OSAS own amphiphilic property, which is favorable to form micelle structure in solution and load much hydrophobic molecules such as HTN (Lu et al., 2019). A higher content of amylose in starch might make its structure more linear and expanding, thus offering more opportunity for starch to react with OSA (as shown in elevated DS) and making OSAS more amphiphilic to load more HTN. This verified the previous speculation that starch with a higher amylose content might have a better solubilizing effect on HTN. Based on the current results, the two samples (OSA-WS-HTN complex and OSA-HAS-HTN complex) with the lowest and highest solubilizing efficacies on HTN were selected for further experiments in this study.

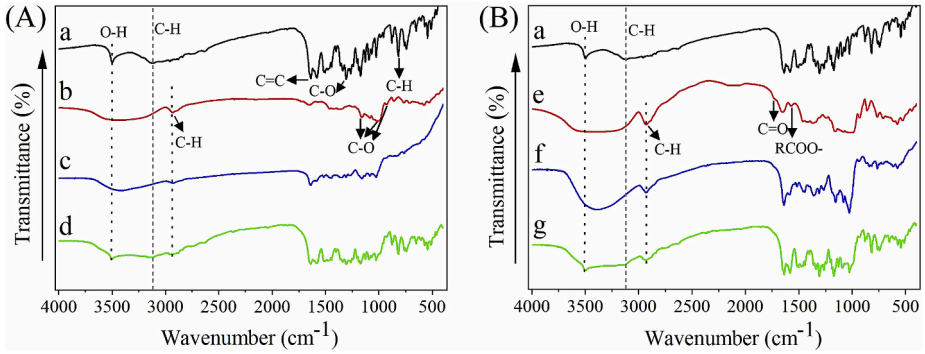

Fig. 3. FT-IR spectra. A: a (HTN), b (OSA-WS), c (OSA-WS-HTN complex) and d (OSA-WS-HTN physical mixture); B: a (HTN), e (OSA-HAS), f (OSA-HAS-HTN complex) and g (OSA-HAS-HTN physical mixture). HTN: hesperetin; OSA: octenyl succinic anhydride; WS: waxy corn starch; HAS: high amylose corn starch.

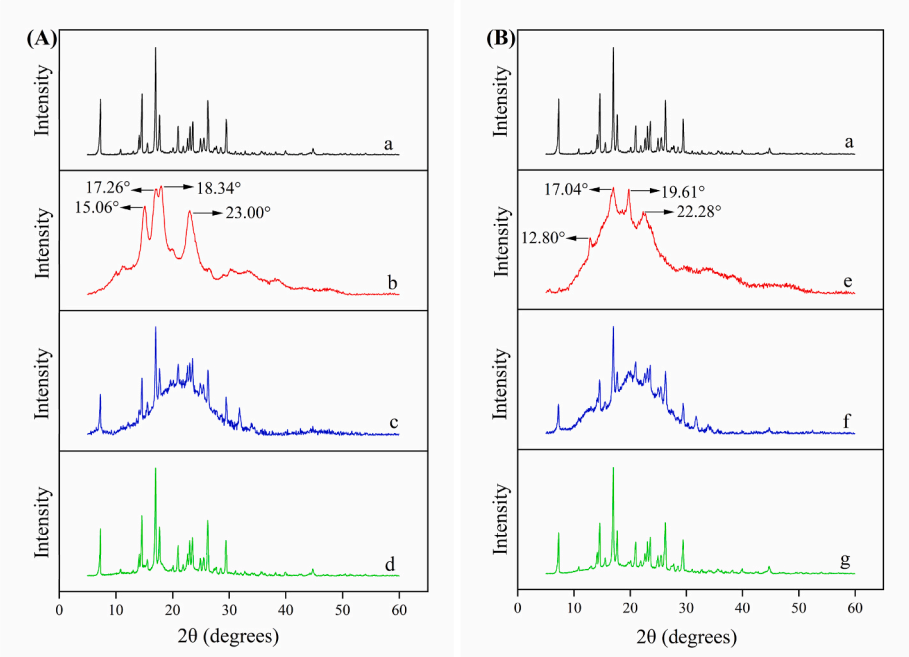

Fig. 4. XRD patterns. A: a (HTN), b (OSA-WS), c (OSA-WS-HTN complex) and d (OSA-WS-HTN physical mixture); B: a (HTN), e (OSA-HAS), f (OSA-HAS-HTN complex) and g (OSA-HAS-HTN physical mixture). HTN: hesperetin; OSA: octenyl succinic anhydride; WS: waxy corn starch; HAS: high amylose corn starch.

3.4. FT-IR analysis

As shown in Fig. 3, the characteristic absorption peak of HTN at 3495 cm^{-1} was the stretching vibration of O–H on the benzene ring, and the characteristic absorption peak of 3115 cm^{-1} corresponded to the C–H vibration on the benzene ring. HTN exhibited prominent absorption peaks in the ranges of 1670–1560, 1465–1230, and 900–800 cm^{-1}, which were attributed to the C═C stretching vibration of the benzene ring, the C–O stretching vibration between the benzene ring and phenolic hydroxy/methoxy groups, and the C–H rocking vibration of the benzene ring, respectively (Guo et al., 2018). The spectra of OSA-WS and OSA-HAS showed strong absorption bands in the range of 3500–3400 cm^{-1}, corresponding to the O–H stretching vibration. The characteristic absorption peak at 2930 cm^{-1} corresponded to C–H stretching vibration, and the discernible peaks at 1157, 1015 and 930 cm^{-1} corresponded to the C–O bond stretching (Ratnaningsih, Harmayani, & Marsono, 2020; Wang et al., 2021). There was no significant difference between the OSA-WS and OSA-HAS samples in the 4000–400 cm^{-1} wavelength range. In addition, the absorption peaks at 1724 and 1570 cm^{-1} represented ester carbonyl and RCOO- of OSA, respectively (Chang et al., 2017). The vibration peaks of the physical mixtures were the superposition of HTN and OSAS, and the characteristic peaks of HTN and OSAS that appeared in the 400–4000 cm^{-1} spectral range could also be observed in the spectra of their physical mixtures. Due to the interference from OSAS, the spectra of OSA-WS-HTN and OSA-HAS-HTN complexes did not contain all the characteristic peaks of HTN. The peak strengths of OSAS-HTN complexes were decreased, and the peak features more similar to those of the corresponding OSAS. The O–H vibration of HTN at 3495 cm^{-1} was not visible in the OSAS-HTN complexes' spectrogram, indicating that HTN was successfully loaded on OSAS. In particular, the peak area ratio of OSA-HAS-HTN to OSA-HAS (2.62) was greater than that of OSA-WS-HTN to OSA-WS (1.01), which also confirmed that OSA-HAS loaded more HTN, and thus had the better solubilization effect on HTN.

3.5. XRD analysis

There were multiple prominent diffraction peaks at 5–30° in the XRD patterns of HTN, indicating a high crystalline structure (see Fig. 4). OSA-WS exhibited typical A-type crystal shape, with diffraction peaks at 15.06°, 17.26°, 18.34° and 23.00° (Obiro, Sinha Ray, & Emmambux, 2012). However, OSA-HAS displayed a typical V-type crystal shape,

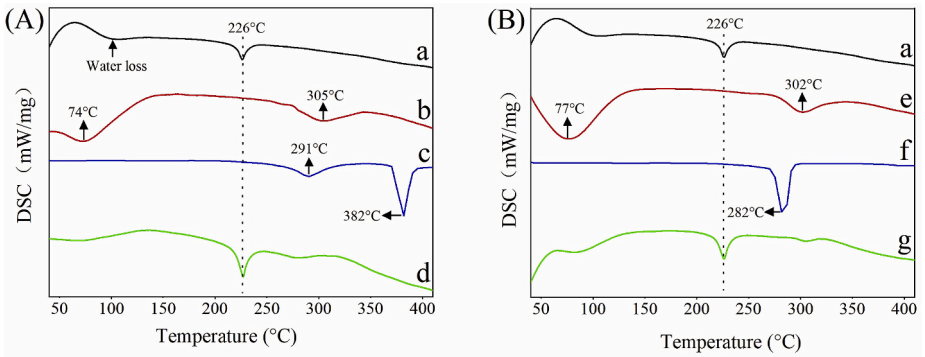

Fig. 5. DSC thermograms. A: a (HTN), b (OSA-WS), c (OSA-WS-HTN complex) and d (OSA-WS-HTN physical mixture); B: a (HTN), e (OSA-HAS), f (OSA-HAS-HTN complex) and g (OSA-HAS-HTN physical mixture). HTN: hesperetin; OSA: octenyl succinic anhydride; WS: waxy corn starch; HAS: high amylose corn starch.

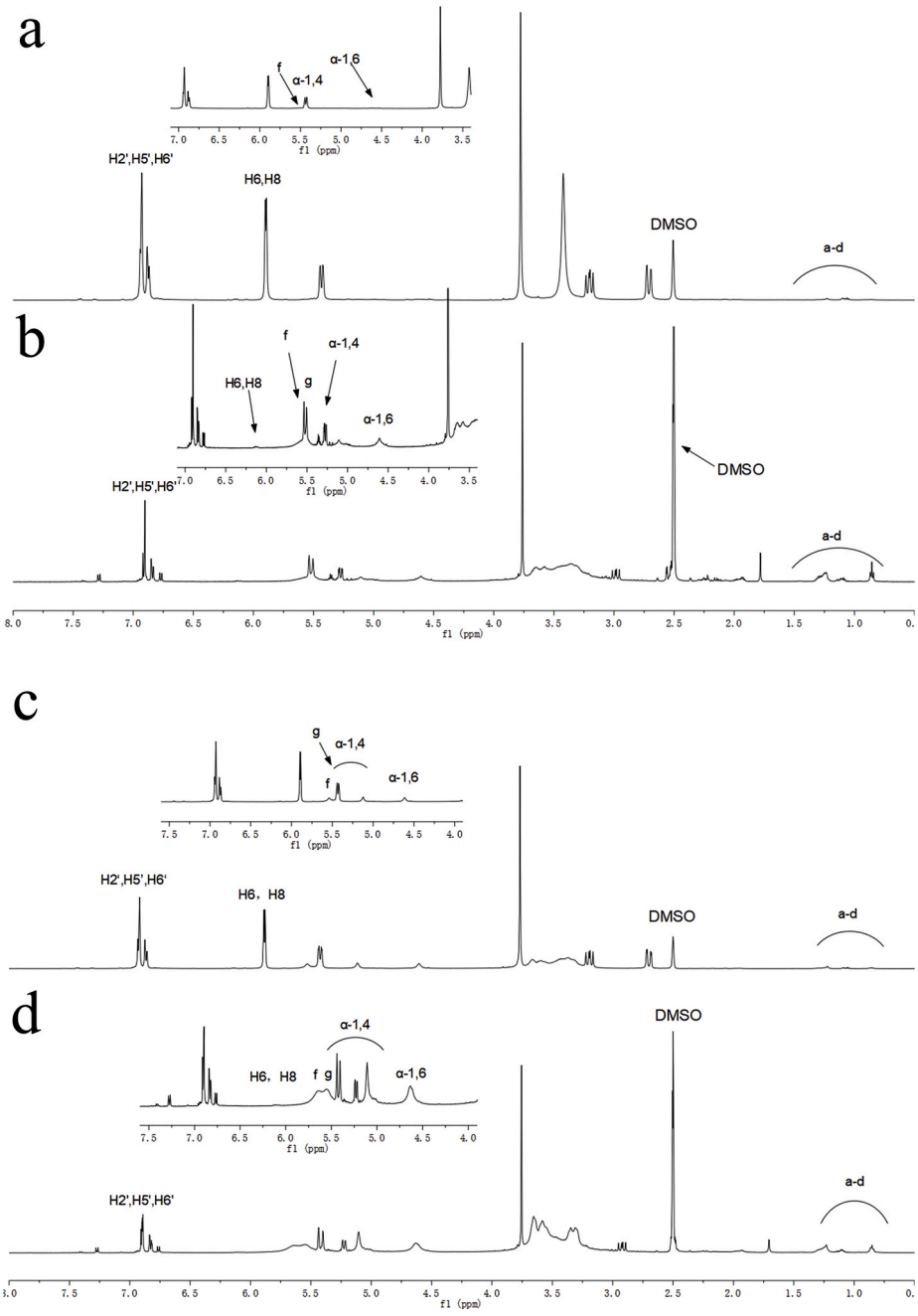

Fig. 6. [1]H NMR spectra. a (OSA-WS-HTN physical mixture), b (OSA-WS-HTN complex), c (OSA-HAS-HTN physical mixture), and d (OSA-HAS-HTN complex). OSA: octenyl succinic anhydride; HTN: hesperetin; WS: waxy corn starch; HAS: high amylose corn starch.

with characteristic diffraction peaks at 12.80°, 17.04°, 19.61° and 22.28°. The XRD patterns of the two physical mixtures mostly displayed the prominent crystal diffraction peaks of HTN. This confirmed that the physical mixtures were mixed mechanically. On the contrary, most crystalline diffraction peaks of HTN vanished in the patterns of the OSAS-HTN complexes, indicating that HTN was mostly integrated into the OSAS, exhibiting an amorphous state (Wang et al., 2021). The decrease of relative crystallinity in the complex represents the increase of HTN solubility. OSA-HAS-HTN complex had a lower relative crystallinity than OSA-WS-HTN complex, indicating that OSA-HAS had a better solubilization effect on HTN, which was consistent with the above experimental results.

3.6. DSC analysis

Fig. 5 showed the thermal properties of the samples. The endothermic peak of HTN at about 100 °C was related to its water loss. The endothermic peak of HTN at 226 °C was attributed to its melting. Due to the water loss of OSAS, the DSC curves of OSA-WS and OSA-HAS displayed large endothermic bands between 40 and 150 °C, with the maximal peaks at 74 and 77 °C, respectively. The thermal decomposition of OSAS induced the endothermic maxima of OSA-WS at 305 °C and OSA-HAS at 302 °C. The endothermic peaks of both HTN and OSAS were present in the two physical mixtures, and the position of the peaks did not vary except for the strength change, indicating that the OSAS and HTN were merely mechanically mixed without any additional covalent or non-covalent interaction between them. In contrast, the endothermic

Table 3
Chemical shifts (ppm) for the protons of hesperetin (HTN) and OSA modified starches (OSAS) in OSAS-HTN complexes and their respective physical mixture.

Chemical shift δ (pmm)	H6, H8 in HTN	H2′, H5′, H6′ in HTN	1, 4 glycosidic bond of starch	1, 6 glycosidic bond of starch	Proton f on OSA group	Proton g on OSA group
OSA-WS-HTN-Physical mixture	5.90	6.93	5.45	4.54	5.53	5.50
OSA-WS-HTN complex	6.15	6.90	5.28	4.60	5.53	5.45
△δ	−0.25	0.03	0.17	−0.06	0.00	0.05
OSA-HAS-HTN-Physical mixture	5.88	6.92	5.44	4.61	5.54	5.44
OSA-HAS-HTN complex	6.12	6.89	5.44	4.64	5.65	5.54
△δ	−0.24	0.03	0.00	−0.03	−0.11	−0.10

OSA: octenyl succinic anhydride; WS: waxy corn starch; HAS: high amylose corn starch.

peak of HTN at 226 °C disappeared in the thermal curves of OSAS-HTN complexes. This indicated that HTN was dispersed in OSAS, and OSAS and HTN formed inclusion complexes. For the OSA-WS-HTN complex, a new endothermic peak was produced at 382 °C, and the dehydration peak of OSA-WS at 291 °C was also visible in the figure. For the OSA-HAS-HTN complex, a new endothermic peak appeared at 282 °C, corresponding to the formation of a new inclusion compound. The peak at this temperature partially coincided with the melting peak of OSA-HAS (302 °C). This demonstrated the interaction between HTN and OSAS, which resulted in the formation of complexes with higher thermal stability.

3.7. ^{1}H NMR analysis

To further explore the mode of interaction between the complexes formed by HTN and OSAS with different amylose and amylopectin compositions, ^{1}H NMR was used to observe the chemical shifts of hydrogen protons in HTN and OSAS in their complexes and physical mixtures, and the results were present in Fig. 6 and Table 3. The chemical shifts of hydrogen protons H6 and H8 in A ring of HTN in the complexes changed more than those of free HTN, indicating that the A ring of HTN interacted mainly with OSAS during the solubilization of HTN by OSAS. The chemical shifts of protons f and g on the OSA group (Fig. 1) are usually around 5.5 ppm (Bai, Shi, Herrera, & Prakash, 2011; Sweedman, Tizzotti, Schäfer, & Gilbert, 2013; Tizzotti, Sweedman, Tang, Schaefer, & Gilbert, 2011), and the chemical shifts of the 1, 4 glycosidic bond and 1, 6 glycosidic bond of starch are 5.1–5.4 ppm and 4.5–5.0 ppm, respectively (Schahl, Lemassu, Jolibois, & Réat, 2022; Wang, Chen, & Liu, 2019; Wang et al., 2021). The value of the displacement difference could reflect the relationship between hydrogen protons of OSAS and HTN. By comparing the chemical shift changes of hydrogen protons on the OSAS main chain and the OSA group, it could be found that the OSA group on OSA-HAS was more involved in the solubilization process of HTN than that on OSA-WS; that was, OSA group in OSAS with high amylose content played a major role in solubilizing HTN, while starch backbone chains in OSA-WS had more interaction with HTN.

4. Conclusions

OSAS with four different amylose and amylopectin compositions had been successfully prepared and their solubilization efficiencies and action modes on HTN were evaluated. The results showed that OSAS with higher content of amylose had a better solubilizing effect on HTN than that with higher amylopectin content. The solubilization efficacy of OSA-HAS on HTN was nearly fivefold that of free HTN, compared to only two folds in OSA-WS. The findings of FT-IR, XRD, DSC, and ^{1}H NMR all indicated the formation of OSAS-HTN complexes. The DSC curves also disclosed that the OSAS-HTN complexes had higher thermal stability. The ^{1}H NMR revealed that the OSA group in OSA-HAS played a major role in the solubilization of HTN, while starch backbone chains in OSA-WS had more interaction with HTN. To summarize, OSA-HAS was discovered to be an excellent solubilizing adjuvant for HTN. In this study, only the structural characteristics, thermal stability and action mode of the OSAS-HTN complexes were explored, with their physicochemical properties receiving less attentions. In the future, the *in vitro* digesting properties, cytotoxicity, and even animal experiments of OSA-HAS and its complex with HTN can be explored to further observe its safety and bioavailability. The solubilizing effect of OSA-HAS and its interaction with other citrus flavonoids (such as hesperidin, naringenin, and naringin) can be investigated. These studies will promote the development of solubilizing or delivering systems for the application of bioactive flavanoids in functional foods or pharmaceuticals.

CRediT authorship contribution statement

Feng Cao: Conceptualization, Formal analysis, Visualization, Writing – review & editing. **Meiyu Zheng:** Conceptualization, Writing – review & editing. **Lu Wang:** Data curation, Methodology, Software, Writing – original draft, Validation. **Hanyu Lu:** Formal analysis, Methodology, Software. **Yangguang Wang:** Conceptualization, Supervision, Validation. **Siew Young Quek:** Supervision, Writing – review & editing. **Shengmin Lu:** Conceptualization, Funding acquisition, Project administration, Validation, Writing – review & editing.

Declaration of competing interest

The authors declare that they have no known competing financial interests or personal relationships that could have appeared to influence the work reported in this paper.

Data availability

Data will be made available on request.

Acknowledgements

The authors acknowledge the National Natural Science Foundation of China (31571892) for the financial support of this research.

References

Abbas, S., Bashari, M., Akhtar, W., Wei, W. L., & Zhang, X. (2014). Process optimization of ultrasound-assisted curcumin nanoemulsions stabilized by OSA-modified starch. *Ultrasonics Sonochemistry, 21*(4), 1265–1274. https://doi.org/10.1016/j.ultsonch.2013.12.017

Altuna, L., Herrera, M. L., & Foresti, M. L. (2018). Synthesis and characterization of octenyl succinic anhydride modified starches for food applications. A review of recent literature. *Food Hydrocolloids, 80*, 97–110. https://doi.org/10.1016/j.foodhyd.2018.01.032

Bai, Y., Shi, Y. C., Herrera, A., & Prakash, O. (2011). Study of octenyl succinic anhydride-modified waxy maize starch by nuclear magnetic resonance spectroscopy. *Carbohydrate Polymers, 83*(2), 407–413. https://doi.org/10.1016/j.carbpol.2010.07.053

Chang, R., Yang, J., Ge, S., Zhao, M., Liang, C., Xiong, L., et al. (2017). Synthesis and self-assembly of octenyl succinic anhydride modified short glucan chains based amphiphilic biopolymer: Micelles, ultrasmall micelles, vesicles, and lutein encapsulation/release. *Food Hydrocolloids, 67*(6), 14–26. https://doi.org/10.1016/j.foodhyd.2016.12.023

Escobar-Puentes, A., Gurrola, A. G., Rincón, S., Zepeda, A., & Martínez-Bustos, F. (2020). Effect of amylose/amylopectin content and succinylation on properties of corn

starch nanoparticles as encapsulants of anthocyanins. *Carbohydrate Polymers, 250*. https://doi.org/10.1016/j.carbpol.2020.116972. Article 116972.
Fang, S., Zhao, X., Liu, Y., Liang, X., & Yang, Y. (2019). Fabricating multilayer emulsions by using OSA starch and chitosan suitable for spray drying: Application in the encapsulation of β-carotene. *Food Hydrocolloids, 93*(8), 102–110. https://doi.org/10.1016/j.foodhyd.2019.02.024
Geng, S., Liu, X., Ma, H., Liu, B., & Liang, G. (2021). Multi-scale stabilization mechanism of pickering emulsion gels based on dihydromyricetin/high-amylose corn starch composite particles. *Food Chemistry, 355*. https://doi.org/10.1016/j.foodchem.2021.129660. Article 129660.
Guo, J., Lu, S., Liu, Z., Tang, W., & Tu, K. (2019). Solubilization of hesperidin with octenyl succinic anhydride modified sweet potato starch. *Food Chemistry, 285*, 180–185. https://doi.org/10.1016/j.foodchem.2019.01.138
Guo, J., Tang, W., Lu, S., Fang, Z., Tu, K., & Zheng, M. (2018). Solubility improvement of hesperetin by using different octenyl succinic anhydride modified starches. *LWT - Food Science and Technology, 95*, 255–261. https://doi.org/10.1016/j.lwt.2018.04.056
Guo, J., Tang, W., Quek, S. Y., Liu, Z., Lu, S., & Tu, K. (2020). Evaluation of structural and physicochemical properties of octenyl succinic anhydride modified sweet potato starch with different degrees of substitution. *Journal of Food Science, 85*(3), 666–672. https://doi.org/10.1111/1750-3841.15031
Hh, A., Hz, B., El, A., Cheng, L. C., & Peng, W. (2019). Structural and functional properties of OSA-starches made with wide-ranging hydrolysis approaches. *Food Hydrocolloids, 90*, 132–145. https://doi.org/10.1016/j.foodhyd.2018.12.011
Ji, X., Du, J., Gu, J., Yang, J., Cheng, L., Li, Z., … Feng, T. (2022). Structure and menthone encapsulation of corn starch modified by octenyl succinic anhydride and enzymatic treatment. *Journal of Food Quality, 2022*. https://doi.org/10.1155/2022/4556827. Article 4556827.
Klaochanpong, N., Puncha-Arnon, S., Uttapap, D., Puttanlek, C., & Rungsardthong, V. (2017). Octenyl succinylation of granular and debranched waxy starches and their application in low-fat salad dressing. *Food Hydrocolloids, 66*(MAY), 296–306. https://doi.org/10.1016/j.foodhyd.2016.11.039
Kuzhithariel Remanan, M., & Zhu, F. (2022). Encapsulation of rutin in Pickering emulsions stabilized using octenyl succinic anhydride (OSA) modified quinoa, maize, and potato starch nanoparticles. *Food Chemistry*. https://doi.org/10.1016/j.foodchem.2022.134790. Article 134790.
Lazer, L. M., Sadhasivam, B., Palaniyandi, K., Muthuswamy, T., Ramachandran, I., Balakrishnan, A., … Ramalingam, S. (2018). Chitosan-based nano-formulation enhances the anticancer efficacy of hesperetin. *International Journal of Biological Macromolecules, 107*, 1988–1998. https://doi.org/10.1016/j.ijbiomac.2017.10.064
Li, H., Ma, Y., Yu, L., Xue, H., Wang, Y., Chen, J., et al. (2020). Construction of octenyl succinic anhydride modified porous starch for improving bioaccessibility of beta-carotene in emulsions. *RSC Advances, 10*(14), 8480–8489. https://doi.org/10.1039/c9ra10079b
Lin, L., Guo, D., Zhao, L., Zhang, X., Wang, J., Zhang, F., et al. (2016). Comparative structure of starches from high-amylose maize inbred lines and their hybrids. *Food Hydrocolloids, 52*(JAN.), 19–28. https://doi.org/10.1016/j.foodhyd.2015.06.008
Liu, F., Sun, L., You, G., Liu, H., Ren, X., & Wang, M. (2020). Effects of Astragalus polysaccharide on the solubility and stability of 15 flavonoids. *International Journal of Biological Macromolecules, 143*, 873–880. https://doi.org/10.1016/j.ijbiomac.2019.09.148
Lucas-Abellán, C., Pérez-Abril, M., Castillo, J., Serrano, A., Mercader, M. T., Fortea, M. I., … Núñez-Delicado, E. (2019). Effect of temperature, pH, β- and HP-β-cds on the solubility and stability of flavanones: Naringenin and hesperetin. *LWT - Food Science and Technology, 108*, 233–239. https://doi.org/10.1016/j.lwt.2019.03.059
Lu, X., Chen, J., Guo, Z., Zheng, Y., Rea, M. C., Su, H., … Miao, S. (2019). Using polysaccharides for the enhancement of functionality of foods: A review. *Trends in Food Science and Technology, 86*, 311–327. https://doi.org/10.1016/j.tifs.2019.02.024
Obadi, M., Qi, Y., & Xu, B. (2022). High-amylose maize starch: Structure, properties, modifications and industrial applications. *Carbohydrate Polymers, 299*. https://doi.org/10.1016/j.carbpol.2022.120185. Article 120185.
Obiro, W. C., Sinha Ray, S., & Emmambux, M. N. (2012). V-amylose structural characteristics, methods of preparation, significance, and potential applications. *Food Reviews International, 28*(4), 412–438. https://doi.org/10.1080/87559129.2012.660718
Paramera, E. I., Konteles, S. J., & Karathanos, V. T. (2011). Stability and release properties of curcumin encapsulated in *Saccharomyces cerevisiae*, β-cyclodextrin and modified starch. *Food Chemistry, 125*(3), 913–922. https://doi.org/10.1016/j.foodchem.2010.09.071
Ratnaningsih, N., Harmayani, E., & Marsono, Y. (2020). Physicochemical properties, *in vitro* starch digestibility, and estimated glycemic index of resistant starch from cowpea (*Vigna unguiculata*) starch by autoclaving-cooling cycles. *International Journal of Biological Macromolecules, 142*, 191–200. https://doi.org/10.1016/j.ijbiomac.2019.09.092
Schahl, A., Lemassu, A., Jolibois, F., & Réat, V. (2022). Evidence for amylose inclusion complexes with multiple acyl chain lipids using solid-state NMR and theoretical approaches. *Carbohydrate Polymers, 276*. https://doi.org/10.1016/j.carbpol.2021.118749. Article 118749.
Shogren, R. L., Viswanathan, A., Felker, F., & Gross, R. A. (2000). Distribution of octenyl succinate groups in octenyl succinic anhydride modified waxy maize starch. *Starch - Strke, 52*(6–7), 196–204. https://doi.org/10.1002/1521-379X (200007)52:6/7.
Sweedman, M. C., Tizzotti, M. J., Schäfer, C., & Gilbert, R. G. (2013). Structure and physicochemical properties of octenyl succinic anhydride modified starches: A review. *Carbohydrate Polymers, 92*(1), 905–920. https://doi.org/10.1016/j.carbpol.2012.09.040
Tizzotti, M. J., Sweedman, M. C., Tang, D., Schaefer, C., & Gilbert, R. G. (2011). New ^{1}H NMR procedure for the characterization of native and modified food-grade starches. *Journal of Agricultural and Food Chemistry, 59*(13), 6913–6919. https://doi.org/10.1021/jf201209z
Tommasini, S., Raneri, D., Ficarra, R., Calabrò, M. L., Stancanelli, R., & Ficarra, P. (2004). Improvement in solubility and dissolution rate of flavonoids by complexation with β-cyclodextrin. *Journal of Pharmaceutical and Biomedical Analysis, 35*(2), 379–387. https://doi.org/10.1016/s0731-7085(03)00647-2
Uchiyama, H., Ando, T., Kadota, K., & Tozuka, Y. (2021). The formation of an amorphous composite between flavonoid compounds: Enhanced solubility in both oil components and aqueous media. *Journal of Drug Delivery Science and Technology, 62*. https://doi.org/10.1016/j.jddst.2021.102410. Article 102410.
Vaz, V. M., Jitta, S. R., Verma, R., & Kumar, L. (2021). Hesperetin loaded proposomal gel for topical antioxidant activity. *Journal of Drug Delivery Science and Technology, 66*. https://doi.org/10.1016/j.jddst.2021.102873. Article 102873.
Wang, K., Cheng, L., Li, Z., Li, C., Hong, Y., & Gu, Z. (2022). The degree of substitution of OSA-modified starch affects the retention and release of encapsulated mint flavour. *Carbohydrate Polymers, 294*. https://doi.org/10.1016/j.carbpol.2022.119781. Article 119781.
Wang, C., Chen, X., & Liu, S. (2019). Encapsulation of tangeretin into debranched-starch inclusion complexes: Structure, properties and stability. *Food Hydrocolloids, 100*. https://doi.org/10.1016/j.foodhyd.2019.105409. Article 105409.
Wang, Y., Zhang, Y., Guan, L., Wang, S., Zhang, J., Tan, L., … Zhang, H. (2021). Lipophilization and amylose inclusion complexation enhance the stability and release of catechin. *Carbohydrate Polymers, 269*. https://doi.org/10.1016/j.carbpol.2021.118251. Article 118251.
Xiang, L., Lu, S., Quek, S. Y., Liu, Z., Wang, L., Zheng, M., … Yang, Y. (2021). Exploring the effect of OSA-esterified waxy corn starch on naringin solubility and the interactions in their self-assembled aggregates. *Food Chemistry, 342*. https://doi.org/10.1016/j.foodchem.2020.128226. Article 128226.
You, G. J., Sun, L. L., Cao, X. X., Li, H. H., Wang, M., Liu, Y. N., et al. (2018). Comprehensive evaluation of solubilization of flavonoids by various cyclodextrins using high performance liquid chromatography and chemometry. *LWT - Food Science and Technology, 94*, 172–177. https://doi.org/10.1016/j.lwt.2018.04.035
Zhang, S., Li, H., Li, M., Chen, G., Ma, Y., Wang, Y., et al. (2022). Construction of ferulic acid modified porous starch esters for improving the antioxidant capacity. *RSC Advances, 12*(7), 4253–4262. https://doi.org/10.1039/d1ra08172a
Zhao, S., Tian, G., Zhao, C., Lu, C., Bao, Y., Liu, X., et al. (2018). Emulsifying stability properties of octenyl succinic anhydride (OSA) modified waxy starches with different molecular structures. *Food Hydrocolloids, 85*(12), 248–256. https://doi.org/10.1016/j.foodhyd.2018.07.029
Zheng, M., Lu, S., & Xing, J. (2021). Enhanced antioxidant, anti-inflammatory and α-glucosidase inhibitory activities of citrus hesperidin by acid-catalyzed hydrolysis. *Food Chemistry, 336*(25). https://doi.org/10.1016/j.foodchem.2020.127539. Article 127539.
Zhu, T., Jackson, D. S., Wehling, R. L., & Geera, B. (2008). Comparison of amylose determination methods and the development of a dual wavelength iodine binding technique. *Cereal Chemistry, 85*(1), 51–58. https://doi.org/10.1094/cchem-85-1-0051

Glossary

HTN: Hesperetin
OSA: Octenyl succinic anhydride
CS: Corn starch
WS: Waxy corn starch
AS: Amylose corn starch
HAS: High amylose corn starch
DS: Degree of substitution
Mw: Molecular weight
CD: Cyclodextrin
OSA-WS: Octenyl succinic anhydride modified waxy corn starch
OSA-HAS: Octenyl succinic anhydride modified high amylose corn starch
OSAS: Octenyl succinic anhydride modified starches
OSAS-HTN: Complexes of octenyl succinic anhydride modified starch and hesperetin
FT-IR: Fourier transform infrared spectroscopy
XRD: X-ray diffraction
DSC: Differential scanning calorimetry
^{1}H NMR: ^{1}H nuclear magnetic resonance